Self-Similar Blow-Up in Nonlinear PDEs

Chris Budd
Othmar Koch
Ewa Weinmüller

AURORA TR2004-15

Institute for Analysis and Scientific Computing
Vienna University of Technology
Wiedner Hauptstrasse 8-10, A-1040 Wien, Austria

E-Mail:cjb@maths.bath.ac.uk
othmar@othmar-koch.org
e.weinmueller@tuwien.ac.at

The work described in this report was supported by the Special Research Program SFB F011 "AURORA" of the Austrian Science Fund FWF.

Introduction

In this report we describe boundary value problems in ordinary differential equations arising in the computation of self-similar blow-up solutions of partial differential equations. In particular, we consider the nonlinear Schrödinger equation, high-order semi-linear parabolic equations, quasi-linear parabolic equations, and the complex Ginzburg-Landau equation. In each case, the problem of the computation of self-similar solutions describing a blow-up in finite time occurring at a single point, is reduced to a nonlinear, ordinary differential equation on an unbounded domain. We discuss the approaches used in the literature and propose new computational methods which show some potential to enhance the efficiency of the computations. Particularly, we discuss the possibility to use our MATLAB solver `sbvp` in the solution process, see [3].

Chapter 1

The Nonlinear Schrödinger Equation

1.1 The Original PDE

The classical nonlinear Schrödinger equation occurs in various important applications in nonlinear optics [17] or plasma physics [29]. The original, partial differential equation in dimension d takes the form

$$\mathrm{i}\frac{\partial u}{\partial t} + \Delta u + |u|^2 u = 0, \quad t > 0, \tag{1.1a}$$

$$u(x,0) = u_0(x), \quad x \in \mathbb{R}^d. \tag{1.1b}$$

In the well-studied case $d = 1$, the equation is integrable and a solution exists globally. For $d \geq 2$, (1.1) has solutions that become unbounded in a finite time T. In this case, the solution becomes infinite at a single point x (without restriction of generality we assume that x is the origin) at which there is a growing and increasingly narrow peak. In plasma physics, the singularity is usually called a collapse, and in nonlinear optics, the singularity corresponds to the phenomenon of self-focussing. In physical applications, we are usually interested in the case $d = 3$. In this case, it is conjectured that the solutions blow up in a self-similar way [13]. We will derive ordinary differential equations which determine the shape of the solution near the blow-up time in the next section. To derive boundary conditions for these ODEs, we note that (1.1) is a unitary Hamiltonian PDE and during the evolution of the solution $u(x,t)$, both the mass M and Hamiltonian H are invariant, that is

$$\frac{dM}{dt} = \frac{dH}{dt} = 0,$$

where

$$M = \int_{\mathbb{R}^3} |u(x,t)|^2 \, dx, \tag{1.2}$$

$$H = \int_{\mathbb{R}^3} \left(|\nabla_x u(x,t)|^2 - \frac{1}{2}|u(x,t)|^4 \right) dx. \tag{1.3}$$

Usually, we will restrict ourselves to the computation of radially symmetric solutions.

1.2 The Associated ODE

The nonlinear Schrödinger equation (1.1) is invariant under four symmetry groups: Translation in time or space, a particular scaling transformation and shift in phase. More precisely, the following changes of variable leave (1.1a) invariant for all $\lambda > 0$:

1. $t \to t + \lambda$,
2. $x \to x + y, \quad \forall y \in \mathbb{R}^d$,
3. $t \to \lambda t,\ x \to \sqrt{\lambda} x,\ u \to \frac{1}{\sqrt{\lambda}} u$,
4. $u \to \mathrm{e}^{\mathrm{i}\lambda} u$.

This does not mean, however, that all the solutions of (1.1) are invariant under the same transformations. Disregarding the first two trivial invariance groups, we are interested in the computation of solutions which are invariant under the two latter transformations. These *self-similar solutions* are usually of great physical importance, because they may be stable attractors for solutions computed from perturbed initial data. Naturally, we are only interested in solutions that give meaningful definitions of the invariants (1.2) and (1.3). Moreover, we restrict ourselves to radially symmetric solutions. Self-similarity can only be expected to hold near blow-up, so for t close to T and x near the origin (that is, $r \approx 0$ for $r = |x|$), we make the ansatz

$$u(x,t) = \frac{1}{\sqrt{2a(T-t)}} \mathrm{e}^{-\mathrm{i}/2a \log(T-t)} z\left(\frac{r}{\sqrt{2a(T-t)}}\right). \tag{1.4}$$

Here, a is a real parameter which expresses the coupling between the phase and the amplitude of u. a is determined simultaneously with the shape function z. Substitution of the ansatz (1.4) into (1.1a) now yields an ODE for z. With the change of variable

$$\tau := \frac{r}{\sqrt{2a(T-t)}},$$

this results in

$$z''(\tau) + \frac{d-1}{\tau} z'(\tau) - z(\tau) + \mathrm{i}a(\tau z(\tau))' + |z(\tau)|^2 z(\tau) = 0, \quad \tau > 0. \tag{1.5}$$

We now derive the boundary conditions for (1.5) which yield a well-posed problem for the computation of z and a with a physically meaningful solution. First, due to symmetry we require

$$z'(0) = 0. \tag{1.6}$$

Moreover, since the phase of z is arbitrary according to the ansatz (1.4),

$$\Im(z(0)) = 0. \tag{1.7}$$

Furthermore, we are interested in solutions u of (1.1a) which decay for $x \to \infty$ [12], [13],

$$z(\infty) = 0. \tag{1.8}$$

This implies that $|z|$ is small for large τ. Consequently, it is possible to discuss the asymptotics of a physically meaningful solution and associated boundary conditions by neglecting the nonlinear part and studying the linear system

$$z''(\tau) + \frac{d-1}{\tau} z'(\tau) - z(\tau) + \mathrm{i}a(\tau z(\tau))' = 0, \quad \tau > 0. \tag{1.9}$$

The fundamental solution modes of this problem are asymptotic to

$$\varphi_1(\tau) = \frac{1}{\tau} \mathrm{e}^{-\mathrm{i}/a \log(\tau)}, \tag{1.10}$$

$$\begin{aligned} \varphi_2(\tau) &= \frac{1}{\tau^{d-1}} \mathrm{e}^{-\mathrm{i}a\tau^2/2 + \mathrm{i}/a \log(\tau)} \\ &= \frac{1}{\tau^2} \mathrm{e}^{-\mathrm{i}a\tau^2/2 + \mathrm{i}/a \log(\tau)} \end{aligned} \tag{1.11}$$

for $\tau \to \infty$ [12].

Subsequently, we refer to solutions of (1.1a) corresponding to φ_1 as *slowly varying*, while those solutions associated with φ_2 are denoted as *rapidly varying*. This reflects the frequency of the oscillations of these fundamental modes for large τ.

Naturally, we are only interested in solutions of (1.9) such that for the associated solution of (1.1) H from (1.3) is finite. This condition translates to

$$H(z) = \int_0^\infty \left(|z'(\tau)|^2 - \frac{1}{2} |z(\tau)|^4 \right) \tau^{d-1} \, d\tau = 0. \tag{1.12}$$

We can choose a constant $c \in \mathbb{C}$ such that the fundamental mode $c\varphi_1$ satisfies this relation, while H is unbounded for the self-similar solution u of (1.1) associated with φ_2. Consequently, the boundary conditions must be posed such as to eliminate contributions from φ_2 from the general solution of (1.9). It turns out that (1.12) is equivalent to the algebraic relation

$$\lim_{\tau \to \infty} \left| \tau z'(\tau) + \left(1 + \frac{\mathrm{i}}{a} \right) z(\tau) \right| = 0, \tag{1.13}$$

see [13]. This relation is indeed satisfied by φ_1, while this condition is violated by φ_2.

Finally, we note that (1.13) can be rewritten, taking into account (1.8). Conditions (1.8) and (1.13) can be summed up as

$$\lim_{\tau\to\infty} \tau z'(\tau) = 0. \tag{1.14}$$

It is important to point out that this last relation is again satisfied by φ_1, but not by φ_2, for which the expression remains bounded, but does not have a limit for $\tau \to \infty$. Consequently, the asymptotic boundary condition (1.14) singles out the slowly varying fundamental mode present in (1.9) and eliminates the rapidly varying mode, as desired.

The boundary value problem that we need to solve for the computation of the self-similar blow-up solution profile is

$$z''(\tau) + \frac{d-1}{\tau} z'(\tau) - z(\tau) + \mathrm{i}a(\tau z(\tau))' + |z(\tau)|^2 z(\tau) = 0, \quad \tau > 0, \tag{1.15a}$$

$$z'(0) = 0, \ \Im z(0) = 0, \ \lim_{\tau\to\infty} \tau z'(\tau) = 0. \tag{1.15b}$$

If we treat the real and imaginary parts of (1.15) separately, we thus need to compute the solutions of two second order differential equations and one real parameter, using five boundary conditions (1.15b). If we augment the system by the trivial equation

$$a'(\tau) = 0, \tag{1.16}$$

we obtain a well-posed boundary value problem for a system of real ordinary differential equations.

1.3 Transformed ODE

Using the Euler transformation $z \to (z, \tau z') = (z_1, z_2)$ for (1.15a), we derive the equivalent first-order equation

$$z'(\tau) = \frac{M(\tau)}{\tau} z(\tau) + f(\tau, z(\tau)), \tag{1.17}$$

where

$$M(\tau) = \begin{pmatrix} 0 & 1 \\ \tau^2(1-\mathrm{i}a) & 2-d-\mathrm{i}a\tau^2 \end{pmatrix}, \ f(\tau, z) = \begin{pmatrix} 0 \\ -\tau z_1 |z_1|^2 \end{pmatrix}.$$

This is an ODE with a singularity of the first kind at $\tau = 0$ and a singularity of the second kind (essential singularity) at $\tau = \infty$. For this reason, we split the interval $(0, \infty]$ into the subintervals $(0, 1]$ and $[1, \infty)$, and require the solution to

be continuous at $\tau = 1$. The problem on $[1, \infty)$ is then transformed to $(0, 1]$ by the substitution $\tau \to 1/\tau$. This yields the four-dimensional BVP

$$z'(\tau) = \begin{pmatrix} \frac{M(\tau)}{\tau} & 0 \\ 0 & \frac{A(\tau)}{\tau^3} \end{pmatrix} z(\tau) + \begin{pmatrix} f(\tau, z_1, z_2) \\ g(\tau, z_3, z_4) \end{pmatrix}, \tag{1.18}$$

where

$$A(\tau) = \begin{pmatrix} 0 & -\tau^2 \\ \mathrm{i}a - 1 & \mathrm{i}a - \tau^2(2-d) \end{pmatrix}, \; g(\tau, z_3, z_4) = \begin{pmatrix} 0 \\ \frac{1}{\tau^3} z_3 |z_3|^2 \end{pmatrix}.$$

In the new variables, the boundary conditions translate to

$$z_2(0) = 0, \; \Im z_1(0) = 0, \; z_1(1) = z_3(1), \; z_2(1) = z_4(1), \; z_4(0) = 0. \tag{1.19}$$

We now review the well-posedness of the transformed problem. In particular, the eigenvalues of the matrices $M(0)$ and $A(0)$ determine what sets of boundary conditions are admissible in order to obtain a continuous (isolated) solution of (1.18), see for example [18], [20]. With a similar argument as in Section 1.2, it is sufficient to discuss the linear version of (1.18) where the nonlinear part is neglected, see also [18], [20]. The admissible boundary conditions for the resulting system

$$z'(\tau) = \begin{pmatrix} \frac{M(\tau)}{\tau} & 0 \\ 0 & \frac{A(\tau)}{\tau^3} \end{pmatrix} z(\tau) \tag{1.20}$$

are the same as for (1.18).

The eigenvalues of $M(0)$ are $\lambda_1 = 0$ and $\lambda_2 = 2 - d = -1$. According to [18], the admissible boundary condition for a well-posed problem with a singularity of the first kind associated with the eigenvalue λ_2 is $z_2(0) = 0$. The second condition (associated with eigenvalue λ_1) can be chosen either at the point $\tau = 0$ or $\tau = 1$. The transition conditions $z_1(1) = z_3(1)$ or $z_2(1) = z_4(1)$ are therefore admissible for a well-posed problem.

The eigenvalues of $A(0)$ are $\lambda_3 = 0$ and $\lambda_4 = \mathrm{i}a$. Consider the fundamental solution modes of (1.20) associated with these eigenvalues:

First, we note that the fundamental modes of the constant coefficient system

$$z'(\tau) = \frac{A(0)}{\tau^3} z(\tau) \tag{1.21}$$

are

$$\phi_3(\tau) = 1, \quad \phi_4(\tau) = \mathrm{e}^{-\mathrm{i}a/(2\tau^2)}.$$

ϕ_4, the mode associated with $\lambda_4 = \mathrm{i}a$, is rapidly oscillating and does not have a limit for $\tau \to 0$. It is therefore desirable to eliminate this mode from the

solution. Indeed, if we transform the mode φ_2 from (1.11) analogously as above, the transplant $\tilde{\varphi}_2(\tau) = 1/\tau\varphi_2'(1/\tau)$ satisfies

$$\tilde{\varphi}_2(\tau) = \left(-\mathrm{i}a + \tau^2\left(\frac{\mathrm{i}}{a} - 2\right)\right) \mathrm{e}^{-\mathrm{i}/a\log(\tau)}\mathrm{e}^{-\mathrm{i}a/(2\tau^2)}.$$

Thus, ϕ_4 displays the same behavior as $\tau \to 0$ as the transformed mode $\tilde{\varphi}_2$. Namely, the solution features a rapid oscillation which is not damped as $\tau \to 0$. Consequently, it is possible to eliminate the undesirable solution mode by requiring $z_4(0) = 0$. This demonstrates that this boundary condition is necessary for a well-posed boundary value problem.

ϕ_3, the fundamental solution of (1.21) corresponding to the eigenvalue $\lambda_3 = 0$, is the constant solution, which is not very useful for our purpose. To analyse the situation further, we consider the eigenvalues of $A(\tau)$. It turns out that

$$\begin{aligned}\lambda_3(\tau) &= \left(1 + \frac{\mathrm{i}}{a}\right)\tau^2 + \left(\frac{1}{a^2} + \frac{\mathrm{i}}{a^3}\right)\tau^4 + O(\tau^6),\\ \lambda_4(\tau) &= \mathrm{i}a - \frac{\mathrm{i}}{a}\tau^2 - \left(\frac{1}{a^2} + \frac{\mathrm{i}}{a^3}\right)\tau^4 + O(\tau^6).\end{aligned}$$

If we incorporate an additional term from the expansion of $\lambda_3(\tau)$ into the system

$$z'(\tau) = \frac{A(\tau)}{\tau^3}z(\tau), \tag{1.22}$$

the discussion is reduced to the scalar equation

$$\hat{\phi}_3'(\tau) = \frac{1}{\tau}\left(1 + \frac{\mathrm{i}}{a}\right)\hat{\phi}_3(\tau). \tag{1.23}$$

This relation represents the leading term of (1.22) if we assume that $\hat{E}(\tau) := (E^{-1})'(\tau)E(\tau)$ is smooth, where $E(\tau)$ is the transformation matrix such that $A(\tau) = E(\tau)J(\tau)E^{-1}(\tau)$ with $J(\tau) = \mathrm{diag}(\lambda_3(\tau), \lambda_4(\tau))$. Indeed, a computation

using MAPLE demonstrates that

$$\begin{aligned}
\hat{E}_{1,1}(\tau) &\sim 2\frac{a^2d + \mathrm{i}ad - 3a^2 - 4\mathrm{i}a + 1}{a^4}\tau^3 + O(\tau^5) \\
&= \frac{2 - 2\mathrm{i}a}{a^4}\tau^3 + O(\tau^5), \\
\hat{E}_{1,2}(\tau) &\sim -\frac{2}{\tau} - 2\frac{-4\mathrm{i}a + \mathrm{i}ad + 2}{a^2}\tau + O(\tau^3) \\
&= -\frac{2}{\tau} - \frac{4 - 2\mathrm{i}a}{a^2}, \\
\hat{E}_{2,1}(\tau) &\sim -2\frac{a^2d + \mathrm{i}ad - 3a^2 - 4\mathrm{i}a + 1}{a^4}\tau^3 + O(\tau^5) \\
&= -\frac{2 - 2\mathrm{i}a}{a^4}\tau^3 + O(\tau^5), \\
\hat{E}_{2,2}(\tau) &\sim \frac{2}{\tau} + 2\frac{-4\mathrm{i}a + \mathrm{i}ad + 2}{a^2}\tau + O(\tau^3) \\
&= \frac{2}{\tau} + \frac{4 - 2\mathrm{i}a}{a^2}.
\end{aligned}$$

Equally as (1.23), the terms $\hat{E}_{1,2}$ and $\hat{E}_{2,2}$ feature a singularity of the first kind. However, since the solution mode associated with ϕ_4 is eliminated by the boundary conditions, the terms that are relevant for our discussion are smooth.

The general solution of the first order ODE (1.23) is

$$\hat{\phi}_3(\tau) = c\tau \mathrm{e}^{\mathrm{i}/a\log(\tau)}.$$

This solution satisfies $\hat{\phi}_3(0) = 0$ and consequently the boundary condition at $\tau = 0$ is satisfied. The constant can be fixed by prescribing a condition $\hat{\phi}_3(1) = c$.

To conclude this discussion, we note that the fundamental solution $\hat{\phi}_3$ corresponds to the slowly varying fundamental mode φ_1 from (1.10). The transplant $\tilde{\varphi}_1(\tau) = 1/\tau\varphi_1'(1/\tau)$ satisfies

$$\tilde{\varphi}_1(\tau) = -\tau\left(1 + \frac{\mathrm{i}}{a}\right)\mathrm{e}^{\mathrm{i}/a\log(\tau)}.$$

1.4 Numerical Solution

Two solution methods are proposed in [13] and [12]. Both work on a truncated interval (where the right endpoint of the integration interval is chosen sufficiently large "adaptively" until convergence of the numerical method is observed). In the first case, a certain minimization procedure is employed.

The second algorithm uses collocation for the second order problem on the truncated interval. The code used for this task is COLSYS, see [2]. Suitable initial

guesses for a and the profile of $z(t)$ have to be provided to solve the nonlinear problems.

Using our code `sbvp`, we can solve the problem (1.18), augmented by (1.16) and the boundary conditions (1.19). Alternatively to $z_4(0) = 0$ we could also use the original condition (1.13) in the form

$$z_4(0) + \left(1 + \frac{\mathrm{i}}{a}\right) z_3(0) = 0.$$

Since the (transplant of the) mode $\varphi_2(\tau)$ from (1.11) is eliminated from the general solution, the slowly varying mode decaying for $\tau \to 0$ has to be approximated. Collocation will be shown to work satisfactorily, since the solution mode we are interested in is characterized by (1.23), which features a singularity of the first kind. For this problem class, collocation methods have been analyzed in [5] and [23]. For the same reason, it will turn out that an error estimate based on defect correction using the backward Euler method as an auxiliary scheme works for this particular problem, even though this estimate is not suitable for boundary value problems with an essential singularity in general.

Even though `sbvp` equally works for complex problems, we separate the real and imaginary parts of z and solve a system of nine real first order differential equations with the same number of boundary conditions. Otherwise, it is not clear how to realize the relation (1.7).

In practice, we are faced with some difficulties to compute the collocation solution of (1.18). A suitable initial approximation for the solution of the associated nonlinear algebraic equations has to be carefully chosen. We obtain this approximation in the following way: setting $a = 0.9$ we solve the initial value problem (1.17) on the interval $[t_0, t_{\mathrm{end}}] = [10^{-4}, 100]$ using the starting values $z_1(t_0) = 2,\ z_2(t_0) = 0$. The numerical solution is determined using the MATLAB initial value problem solver `ode15s`. The numerical solution is evaluated at N points which correspond to a uniform mesh $\Delta_h = \{i/N : i = 1, \ldots, N\}$ of the transformed problem (1.18) on $[1/N, 1]$, where the initial points $z_1(0) = 2,\ z_2(0) = 0$ are added to the points determined from the shooting procedure above. The approximation determined from the shooting procedure for (1.17) is given in Figure 1.1. The computations reported in Figures 1.1– 1.5 use a mesh where $N = 3000$.

The initial profile transformed back to the mesh Δ_h for (1.18) is given in Figure 1.2.

Using a moderate tolerance $TolX = 5 \cdot 10^{-3}$ for the increment in the Newton iteration, the numerical solution of (1.18) can now be determined successfully. To this end, we used our collocation solver `sbvpcol` from the package `sbvp`, see [3], which computes the collocation solution on a fixed mesh. Firstly, we use collocation at one Gaussian point, a method of second order. The result is shown in Figure 1.3.

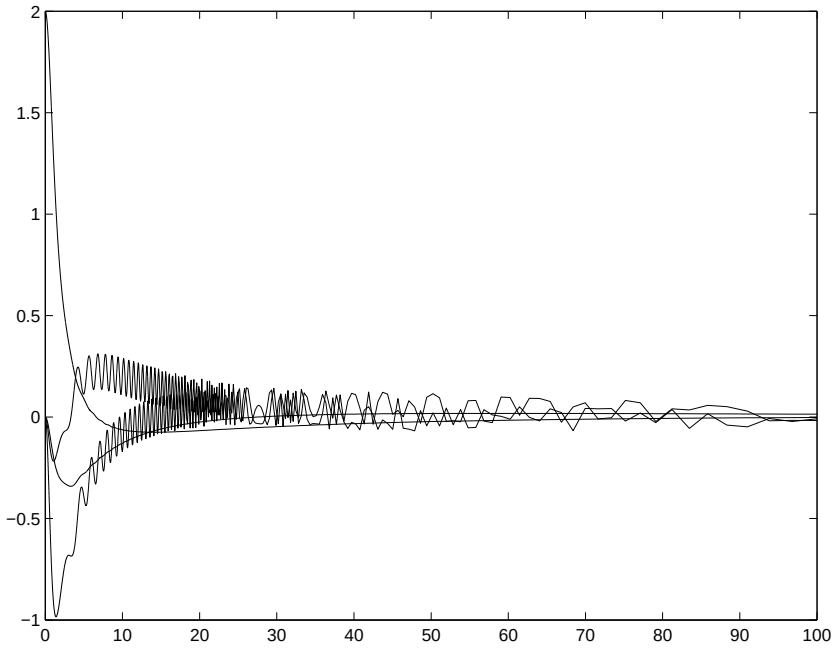

Figure 1.1: Initial profile for (1.17) computed by shooting.

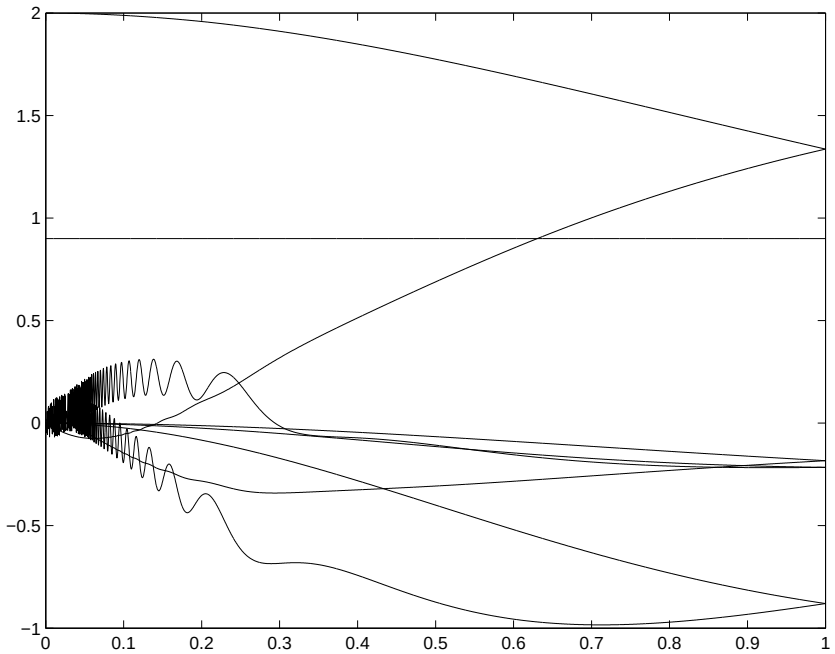

Figure 1.2: Initial profile for (1.18).

Using this numerical solution, we can refine our shooting procedure for the initial profile by setting $z_1(t_0) = 1.88$. The result is given in Figure 1.4.

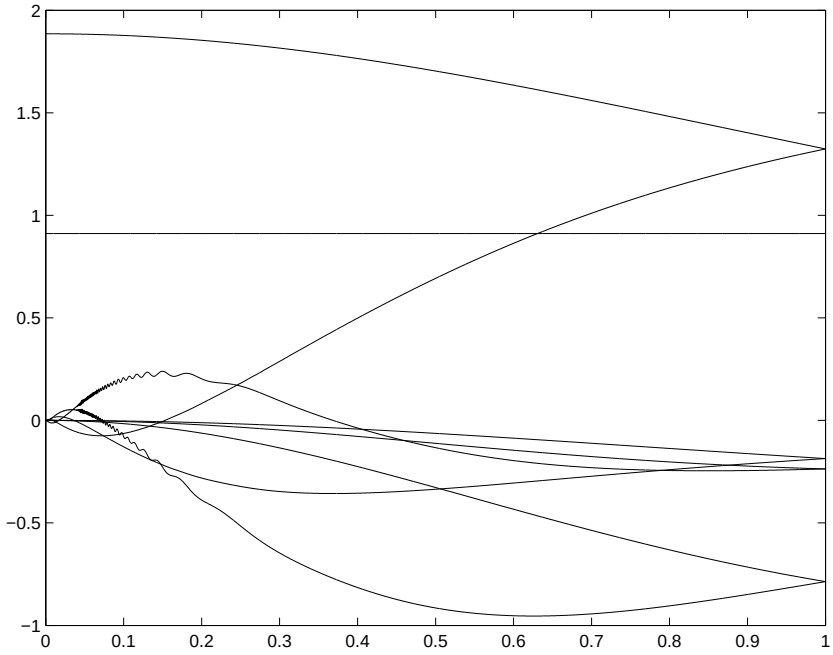

Figure 1.3: Solution of (1.18).

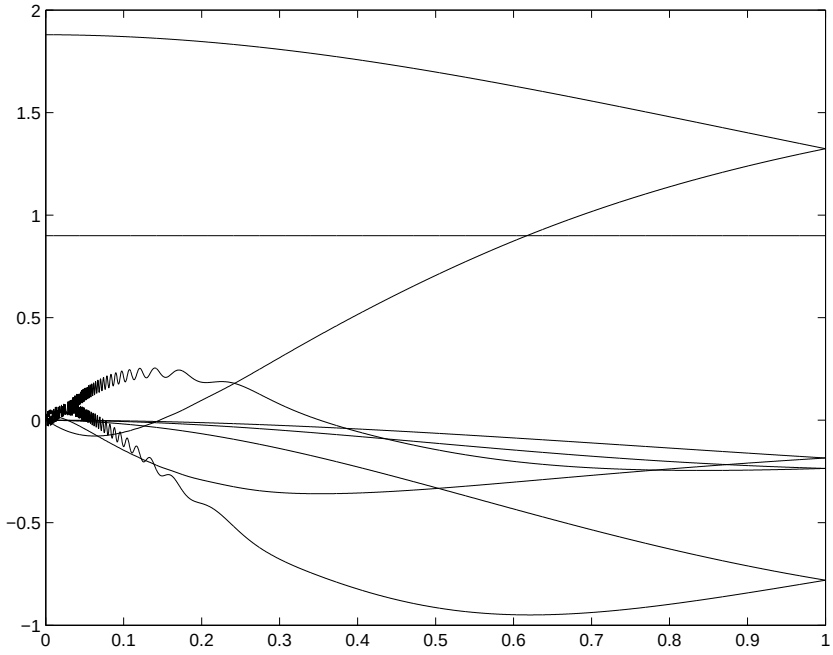

Figure 1.4: Refined initial profile for (1.18).

We note that this refined starting approximation oscillates less strongly than the profile given in Figure 1.2. Obviously, this initial profile resembles the solution of the boundary value problem (1.18) more closely, since the initial value for z_1 is chosen more realistically. Using this refined initial profile, we again obtain a numerical solution from our collocation solver which resembles the result in Figure 1.3, see Figure 1.5.

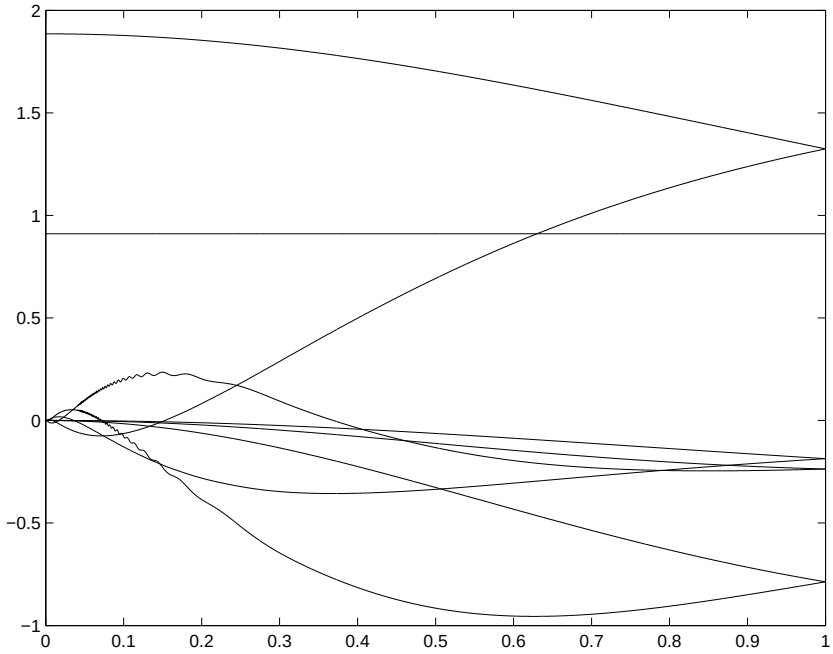

Figure 1.5: Solution of (1.18) using refined initial profile.

So far, we have used a low order collocation method (Gaussian collocation at one point, which is equivalent to the box scheme) on a very fine grid ($N = 3000$) in order to approximate the solution. We can obtain a similar accuracy by using higher order collocation at a coarser grid. In Figure 1.6 we give the result of Gaussian collocation at four points on a mesh with $N = 500$ to illustrate this observation.

In the same setting, we also tried our full code `sbvp` which incorporates error estimation based on defect correction using the backward Euler method as an auxiliary scheme, and mesh adaptation, see [3]. It was demonstrated in [6] that the error estimate in the release version is not suitable for problems with an essential singularity in general. Due to the fact that the solution modes that are actually present in the solution we want to resolve are associated with problems featuring a singularity of the first kind, however, our error estimate appears to work acceptably for (1.18). Indeed, in the same setting as for Figure 1.6 with moderate error tolerances, the solution on the uniform initial grid with $N = 500$ is accepted (and coincides with Figure 1.6, of course).

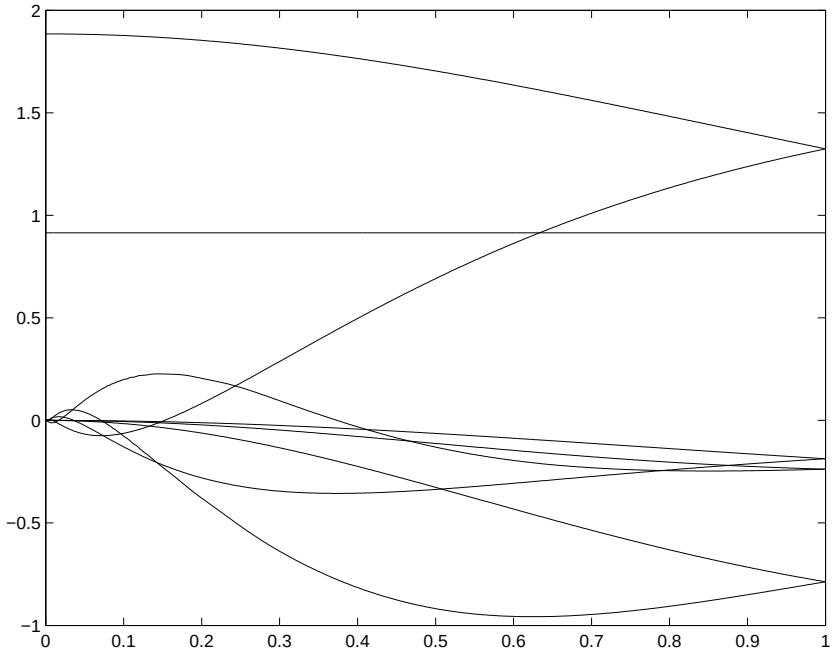

Figure 1.6: Solution of (1.18) computed by high order collocation.

More interestingly, we also tried `sbvp` with a low order method ($m = 1$ Gaussian points, which corresponds to the box scheme), and using an initial grid with $N = 100$ and the initial profile computed for $z_1(t_0) = 2$. The tolerance for the Newton method was chosen as $TolX = 10^{-2}$, and for the mesh selection we used error tolerances $AbsTol = RelTol = 5 \cdot 10^{-3}$. Mesh adaptation did take place in this setting, the tolerances were satisfied on a grid with $N = 256$ and a ratio of 9.71 between the largest and smallest steps in the final mesh. The solution computed thus is close to those computed previously and is displayed in Figure 1.7.

In Figure 1.8, we show a plot of the "exact error" of this numerical approximation (with respect to a reference solution computed using a uniform mesh with $N = 1000$) and compare this with the error estimate computed by `sbvp`. The qualitative behavior of the error seems to be captured quite well, unfortunately the error is underestimated by about a factor of four, see Figure 1.8.

For this low order method, it is even possible to observe experimentally the classic convergence order of the global error. In Table 1.1, we give the empirical convergence order the numerical solutions computed as follows:

For a uniform time grid with step-size h_i, denote the numerical solution by ξ_i. If z is the exact solution and ξ_{i+1} and ξ_{i+2} denote the numerical approximations on

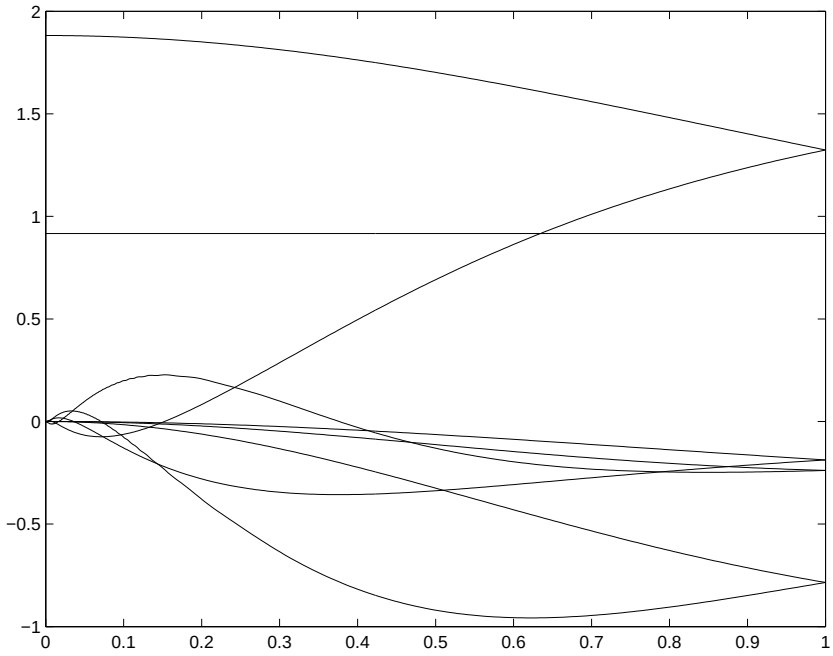

Figure 1.7: Solution of (1.18) computed using `sbvp`.

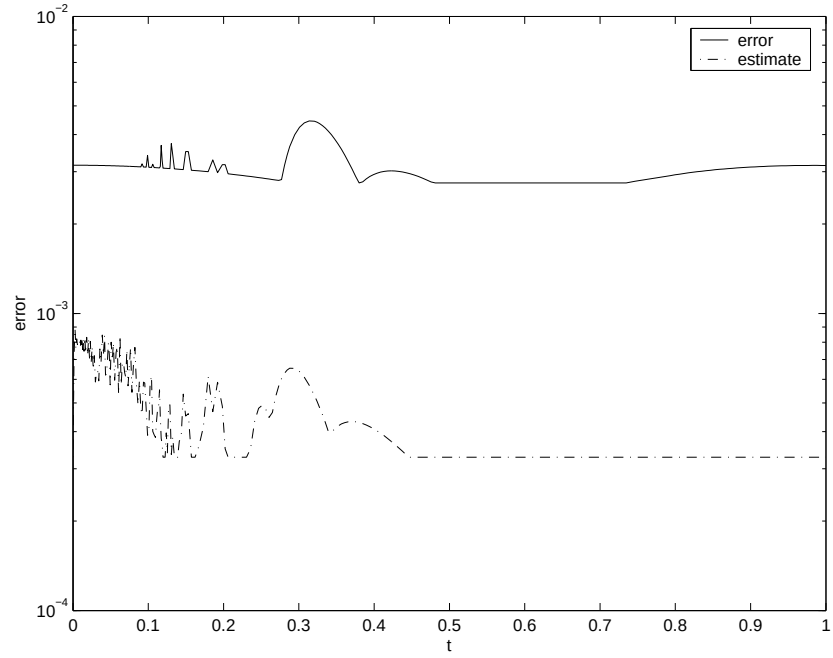

Figure 1.8: Global error and error estimate for (1.18).

grids with step-sizes $h_i/2$ and $h_i/4$, respectively, we assume

$$\begin{aligned} \xi_i - z &\approx Ch_i^p, \\ \xi_{i+1} - z &\approx Ch_i^p \frac{1}{2^p}, \\ \xi_{i+2} - z &\approx Ch_i^p \frac{1}{4^p}, \end{aligned}$$

with some integer p. This implies

$$\begin{aligned} \xi_i - \xi_{i+1} &= Ch_i^p (1 - \frac{1}{2^p}), \\ \xi_{i+1} - \xi_{i+2} &= Ch_i^p (1 - \frac{1}{2^p}) \frac{1}{2^p}. \end{aligned}$$

Consequently, the order p can be estimated empirically as

$$p \approx \frac{\ln\left(\frac{\|\xi_i - \xi_{i+1}\|}{\|\xi_{i+1} - \xi_{i+2}\|}\right)}{\ln(2)},$$

where $\|\cdot\|$ denotes the maximum norm on the space of grid vectors.

Table 1.1 gives, for each equidistant step-size h_{i+1}, the quantities $\|\xi_i - \xi_{i+1}\|$ (denoted by err) (naturally the first row has no entry) and the empirical convergence order p computed as explained above from the values of three consecutive numerical approximations. These are computed using `sbvpcol`, where the starting approximation for Newton's method is computed from an initial value problem with $z(0) = 2$.

h_i	err	p
4.0000e−03		
2.0000e−03	3.3750e−02	
1.0000e−03	8.0415e−03	2.07

Table 1.1: Convergence order for $m = 1$ Gaussian point.

If alternatively we use four equidistant collocation points, we do not observe the classical convergence order, see Table 1.2. There are a few possible reasons for this behavior. The fine spacing between the collocation points might introduce large roundoff errors which govern the error and do not admit to observe the regular behavior of the discretization error. Secondly, Newton's method does not compute the solution of the algebraic equations with very high precision and these errors possibly dominate the discretization error. Finally, it is possible that the exact solution of (1.5) is unsmooth and does not permit a high convergence order of discretization schemes.

h_i	err	p
6.6667e−03		
3.3333e−03	6.0840e−02	
1.6667e−03	2.3271e−02	1.39

Table 1.2: Convergence order for $m = 4$ equidistant collocation points.

1.4.1 Multi-Bump Solutions

The solution of (1.5) we have discussed so far is *stable* and *monotone*, i. e., $|z(\tau)| \to 0$ monotonely as $\tau \to \infty$ (see also Figure 1.9). Consequently, the solution can be approximated numerically comparatively easily. In [13], it was shown that in addition, unstable, non-monotone solutions of (1.5) exist. These *multi-bump* solutions are more difficult to resolve. In [13] these profiles were computed by an intricate pathfollowing procedure. Using `sbvpcol`, we could resolve these solutions within certain limitations.

Starting from the branch corresponding to the monotone solution at $d = 2.01$, simple continuation (varying d in equidistant steps of $\Delta d = 0.01$ and using the result from each step as the starting profile for the next step), we were successful in resolving the monotone solution for $d = 3$. Thus, we used our shooting procedure to compute the starting profile at $d = 2.01$ using $z(0) = 2.120627439$ and $a = 0.385950653$ (see [13]), and subsequently approximated the solution for all d on an equidistant grid with $N = 1200$ by using our collocation solver `sbvpcol`. In Figure 1.9, we show the profiles of $|z(\tau)|$ (transformed back to the unbounded interval) for $d = 2.01$ and $d = 3$, and the value of a for $d \in [2.01, 3]$. In the course of the computations, we encountered severe problems in the convergence of our solver for nonlinear algebraic equations (resulting in the unsmooth change in the computed values of a visible in Figure 1.9 for d near 2), finally the stable, monotone solution could be approximated with the same accuracy as in previous experiments.

Trying to follow the solution branch associated with a multi-bump solution, however, proved very difficult with our crude method. Starting at $z(0) = 2.083537069$ and $a = 0.159401767$ for $d = 2.01$ (the solution profile features one local maximum), the convergence problems of our nonlinear solver caused a very irregular behavior near $d = 2$. For larger d, however, the solution profile could be approximated reasonably well. For the solution at $d = 2.01$ and $d = 3$ and the graph of a for $d \in [2.01, 3]$, see Figure 1.10.

If instead of using pathfollowing starting from $d = 2.01$ we start with the solution at $d = 3$ and follow the solution branch to $d = 2.01$, we can avoid the irregular behavior near $d = 2$ in the approximation of the stable, monotone solution. Figure 1.11 gives the solution profiles at the starting point and the end point of

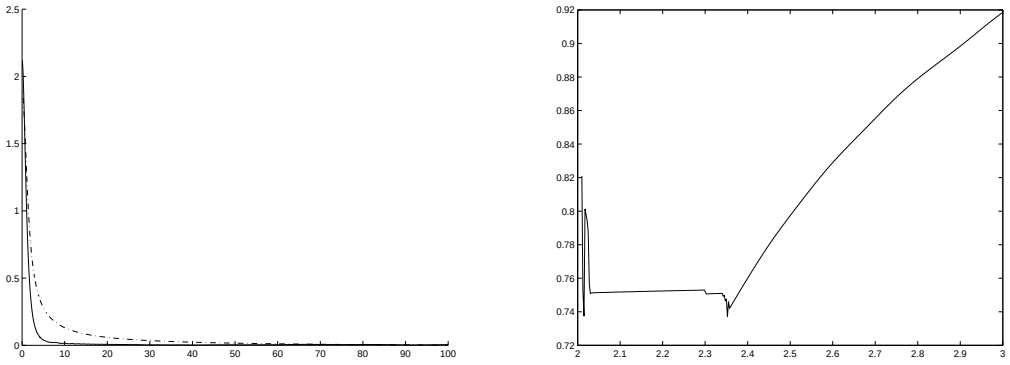

Figure 1.9: $|z(\tau)|$ for $d = 2.01$ and $d = 3$ (left) and a for $d \in [2.01, 3]$.

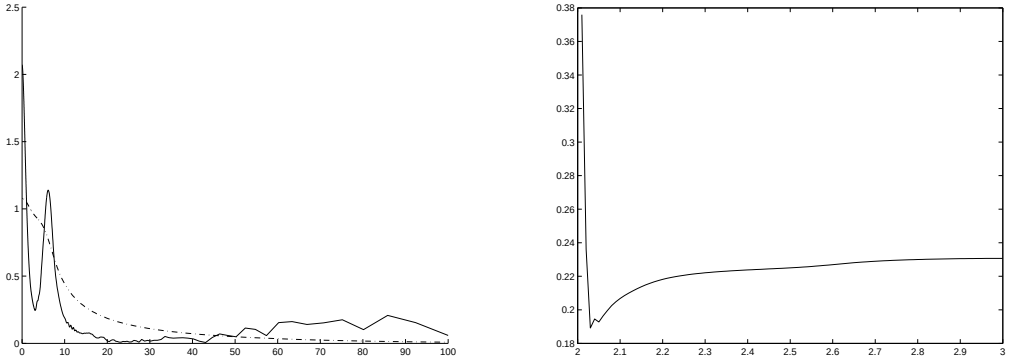

Figure 1.10: $|z(\tau)|$ for $d = 2.01$ and $d = 3$ (left) and a for $d \in [2.01, 3]$.

the path, and the profile of a along this path. Thus, the monotone solution can be approximated very reliably near $d = 2$ using this procedure. Unfortunately, this does not work for the multi-bump solutions. In that case, the solution at $d = 3$ cannot be computed with sufficient accuracy when using shooting to determine a starting profile for the nonlinear equations.

1.4.2 Solution of the Second-Order Equations

It seems attractive to try and solve the equations (1.15) in the second order form, thus reducing the dimension of the resulting system of singular ODEs. However, if we transform (1.15a) to a system of two second-order equations on $[0, 1]$ without using the Euler transformation to reduce the problem to first order, the asymptotic boundary condition $\lim_{\tau\to\infty} \tau z'(\tau)$ cannot be translated into the new variables and the numerical solution is not successful, see [22]. Yet, by using a collocation solver for mixed order systems which is currently being developed, we can successfully compute the solution by using the first order formulation for

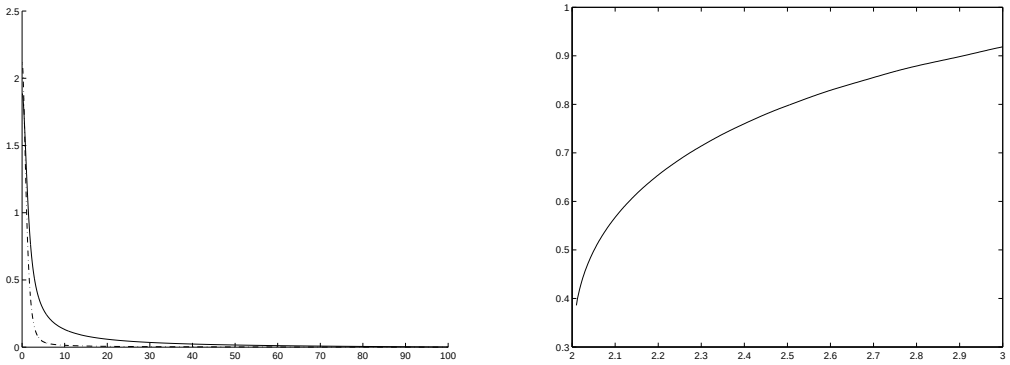

Figure 1.11: $|z(\tau)|$ for $d = 2.01$ and $d = 3$ (left) and a for $d \in [2.01, 3]$.

the interval $[1, \infty)$, the original second order equation for the problem on $[0, 1]$, and we may omit the auxiliary differential equation for the variable a which only appears algebraically in the original problem. For details, see [21].

Chapter 2

High-Order Semi-Linear Parabolic Equations

2.1 The Original PDEs

Here, we discuss the extended Frank-Kamenetskii equation,

$$\frac{\partial u}{\partial t} = (-1)^{m+1}\frac{\partial^{2m} u}{\partial x^{2m}} + \mathrm{e}^u, \quad x \in \mathbb{R},\ t > 0, \tag{2.1}$$

and a similar problem with a polynomial nonlinear part,

$$\frac{\partial u}{\partial t} = (-1)^{m+1}\frac{\partial^{2m} u}{\partial x^{2m}} + |u|^{p-1}u, \quad x \in \mathbb{R},\ t > 0, \tag{2.2}$$

where $m > 1$ is a natural number and $p > 1$. We will focus on the case where $m = 2$. In numerical calculations in [10], $p = 2$ is chosen.

Higher order parabolic equations appear in many relevant applications in thin film theory, convection-explosion theory, lubrication theory, flame and wave propagation (the Kuramoto-Sivashinskii equation and the Fisher-Kolmogorov equation), or self-focussing problems in nonlinear optics ([7], [15]). It is therefore important to study the behavior of the solutions of higher-order extensions of well studied second order equations as in (2.1) and (2.2).

2.2 The Associated ODEs

Similarly as in Section 1.1, we are interested in self-similar solutions of (2.1) and (2.2), respectively [10].

The PDE (2.1) is invariant under the group of transformations

$$t \to \lambda t,\ x \to \lambda^{1/2m} x,\ u \to u - \ln(\lambda), \quad \lambda > 0,$$

while (2.2) is invariant with respect to the scaling transformation

$$t \to \lambda t,\ x \to \lambda^{1/2m} x,\ u \to \lambda^{-1/(p-1)} u, \quad \lambda > 0.$$

Using the new, self-similar space variable

$$\tau := \frac{x}{(T-t)^{1/2m}}, \tag{2.3}$$

we make the ansatz

$$u(x,t) = -\ln(T-t) + z(\tau), \tag{2.4}$$

and

$$u(x,t) = (T-t)^{-1/(p-1)} z(\tau), \tag{2.5}$$

respectively. Substitution into the PDEs (2.1) and (2.2) yields the following ODEs for the functions z:

$$(-1)^{m+1} z^{(2m)}(\tau) - \mu\tau z'(\tau) + \mathrm{e}^{z(\tau)} - 1 = 0, \tag{2.6}$$

and

$$(-1)^{m+1} z^{(2m)}(\tau) - \mu\tau z'(\tau) + |z(\tau)|^{p-1} z(\tau) - \frac{z(\tau)}{p-1} = 0. \tag{2.7}$$

From the ansatz (2.3), $\mu = 1/2m$. For this value of μ we obtain rescaled self-similar profiles.

Due to symmetry, we choose boundary conditions

$$z'(0) = z'''(0) = \cdots = z^{(2m-1)}(0) = 0. \tag{2.8}$$

Our aim is to compute "slowly-growing solutions" of (2.6) and (2.7), respectively. For (2.7), these are characterized by the fact that the terms $-\mu\tau z'(\tau)$ and $-\frac{z(t)}{p-1}$ balance. Consequently, we require

$$\mu\tau z'(\tau) = -\frac{z(\tau)}{p-1}.$$

This means that

$$z(\tau) \sim c\tau^{-1/\mu(p-1)}. \tag{2.9}$$

There are several ways in which this can be translated into boundary conditions at $\tau = \infty$. In [10] the "highest derivatives" of $z(t)$ are set equal to 0 at a large value $T = 1000$. In our framework the resulting relations are

$$z^{(m+1)}(\infty) = \cdots = z^{(2m)}(\infty) = 0. \tag{2.10}$$

However, the asymptotic relation (2.9) also implies that

$$z(\infty) = z'(\infty) = \cdots = z^{(m-1)}(\infty) = 0, \tag{2.11}$$

or actually $z^{(k)}(\infty) = 0$ for any k. Which of these relations are suitable in the framework of the equivalent first-order problem with an essential singularity will be discussed in the next section.

For (2.6), the asymptotic boundary condition at $\tau = \infty$ turns out to imply that z is *slowly growing*, but *not bounded* for growing τ. Consequently, this problem cannot be transformed to a well-posed singular problem on $[0,1]$ and the numerical solution is not possible straightforwardly by using our approach advocated here.

2.3 Transformed ODEs

The standard transformation $z \to (z, z', z'', \ldots, z^{(2m-1)}) = (z_1, \ldots, z_{2m})$ yields

$$z'(\tau) = M(\tau)z(\tau) + f(\tau, z_1(\tau)), \tag{2.12}$$

where

$$M(\tau) = \begin{pmatrix} 0 & & & \\ \vdots & & I_{2m-1} & \\ 0 & & & \\ 0 & (-1)^{m+1}\mu\tau & 0 & \cdots \end{pmatrix}, \; f(\tau, z) = \begin{pmatrix} 0 \\ \vdots \\ 0 \\ (-1)^{m+1}(1 - \mathrm{e}^z) \end{pmatrix},$$

or

$$M(\tau) = \begin{pmatrix} 0 & & & \\ \vdots & & I_{2m-1} & \\ 0 & & & \\ (-1)^m \frac{1}{1-p} & (-1)^{m+1}\mu\tau & 0 & \cdots \end{pmatrix}, \; f(\tau, z) = \begin{pmatrix} 0 \\ \vdots \\ 0 \\ (-1)^m z|z|^{p-1} \end{pmatrix},$$

respectively. Since this a problem posed on $(0, \infty)$, we again split the integration interval at the point $\tau = 1$, where we require the solution to be continuous. The interval $[1, \infty)$ is again transformed to $(0, 1]$ via $\tau \to 1/\tau$ and we obtain the system

$$z'(\tau) = \begin{pmatrix} M(\tau) & 0 \\ 0 & -\frac{1}{\tau^3}N(\tau) \end{pmatrix} z(\tau) + \begin{pmatrix} f(\tau, z_1(\tau)) \\ -\frac{1}{\tau^2} f(\tau, z_{2m+1}(\tau)) \end{pmatrix}, \tag{2.13}$$

where

$$N(\tau) = \begin{pmatrix} 0 & & & \\ \vdots & & \tau I_{2m-1} & \\ 0 & & & \\ 0 & (-1)^{m+1}\mu & 0 & \cdots \end{pmatrix}, \; f(\tau, z) = \begin{pmatrix} 0 \\ \vdots \\ 0 \\ (-1)^{m+1}(1 - \mathrm{e}^{z_1}) \end{pmatrix},$$

or

$$N(\tau) = \begin{pmatrix} 0 & & & \\ \vdots & & \tau I_{2m-1} & \\ 0 & & & \\ (-1)^m \frac{1}{1-p}\tau & (-1)^{m+1}\mu & 0 & \cdots \end{pmatrix}, \; f(\tau, z) = \begin{pmatrix} 0 \\ \vdots \\ 0 \\ (-1)^m z|z|^{p-1} \end{pmatrix},$$

respectively. This formulation reduces the problem to the standard form discussed in [20].

The symmetry conditions (2.8) and the continuity requirements translate to

$$z_2(0) = \cdots = z_{2m}(0) = 0, \; z_j(1) = z_{2m+j}(1), \quad j = 1, \ldots, 2m.$$

The minimal growth conditions (2.10) cannot be expressed in terms of the new variables. It seems natural to replace them by

$$z_{3m+1}(0) = \cdots = z_{4m}(0) = 0. \tag{2.14}$$

Alternatively, we also consider the boundary conditions (2.11), or equivalently

$$z_{2m+1}(0) = \cdots = z_{3m}(0) = 0. \tag{2.15}$$

To discuss the well-posedness of the resulting, first order boundary value problems, we consider the spectrum of the coefficient matrices.

For $m > 1$, the eigenvalues of $N(0)$ for both matrices in (2.13) are all equal to 0, where there exist $2m - 1$ linearly independent eigenvectors and one principal vector. This means that the Jordan canonical form associated with $N(0)$ contains one block of dimension 2 (with a single entry that is equal to 1), and is diagonal otherwise. This case is not discussed in [20], but results from [24] might be adapted for our purpose. It is clear in any case that contributions to the general solution of the linear system

$$z'(\tau) = \frac{N(0)}{\tau^3} z(\tau)$$

which are associated with eigenvectors of $N(0)$ are not critical (at least for the discussion of the analytical properties of the problem), while contributions associated with the principal vector $\tilde{e} = (0, 1, 0, \ldots, 0)^T$ are in general unbounded for $\tau \to 0$. To eliminate these solution modes, we require

$$z_{2m+2}(0) = 0. \tag{2.16}$$

The choice of the remaining boundary conditions

$$z_{2m+k}(0) = 0 \tag{2.17}$$

may be adapted to the requirements of numerical solution methods. It appears practical to use $z_{2m+1}(0) = 0$ to eliminate the trivial solution $z \equiv 1$ of (2.7). This is also the boundary condition used in the numerical experiments reported in the next section.

2.4 Numerical Solution

In [10], continuation using the automatic pseudo-arclength routine AUTO, see [14], is employed to solve (2.7). The initial points on each curve are obtained by

setting $\mu = 0$. The resulting BVPs are solved by `bvp4c` on a truncated interval, see [28]. No numerical solution of the more difficult problem (2.6) is attempted.

After transformation to the form (2.13), we expect `sbvp` to be applicable to solve the problem numerically for any μ. The problem corresponding to (2.6) cannot be solved straightforwardly by the approach outlined here, since the solution to this problem becomes unbounded for $\tau = \infty$.

To illustrate the successful application of our solver, we give the results for $m = 2$ and $\mu = 1/4$ which corresponds to the self-similar solution profile. The nonlinear problem (2.7) has two solutions. In Figure 2.1 we give the starting profile we chose heuristically (defined by a Gaussian function and its derivatives on the original interval $[0, \infty)$), and the solution profile computed for (2.7) (via (2.13)) by our collocation solver `sbvpcol` on an equidistant grid with $N = 500$. In Figure 2.2, we give an alternative starting profile and resulting alternative solution of (2.7). The four solution components given in the figures correspond to the four solution components of (2.12) on the unbounded interval.

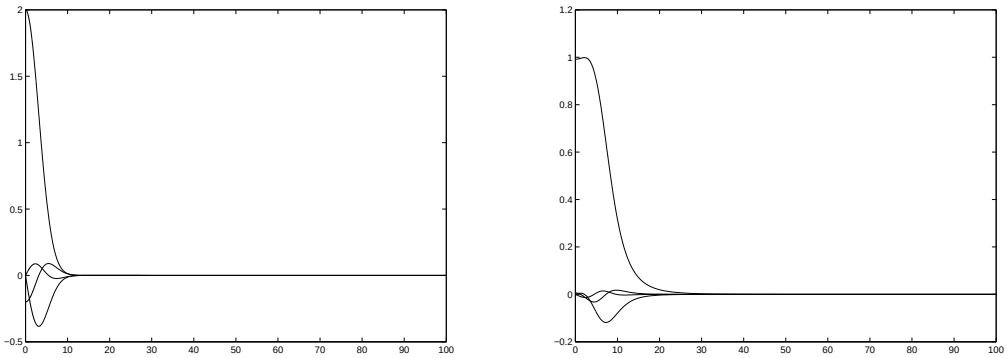

Figure 2.1: Starting profile (left) and $z(\tau)$ (right) for the first solution of (2.12).

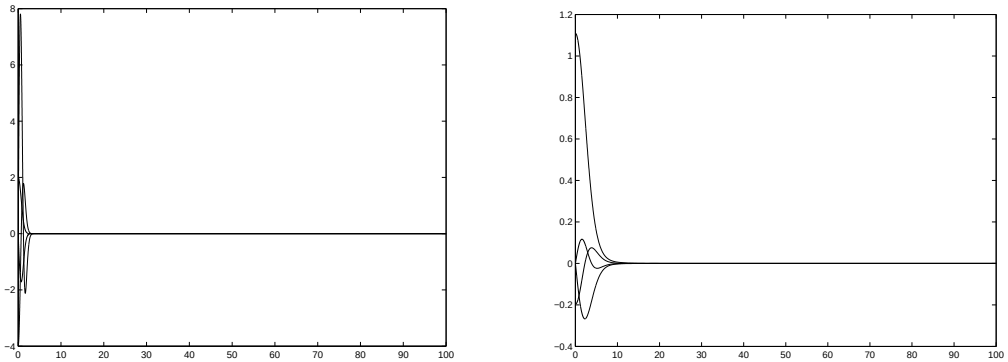

Figure 2.2: Starting profile (left) and $z(\tau)$ (right) for the second solution of (2.12).

Not surprisingly, this problem, in contrast to the nonlinear Schrödinger equation, cannot be solved by our original solver `sbvp 1.0`. The default error estimate based on the backward Euler method fails due to the presence of an essential singularity. If an alternative error estimate, based on defect correction and the box scheme (see [4]), is used, however, the computations by `sbvp` are successful. In Figure 2.3, we show the eight solution components of (2.13), where the solution given in Figure 2.2 is approximated. Using an initial mesh with $N = 20$, the solution is approximated with accuracy $AbsTol = RelTol = 10^{-7}$. The final mesh contains 73 points, and the ratio between the largest and the smallest stepsize is 1.86.

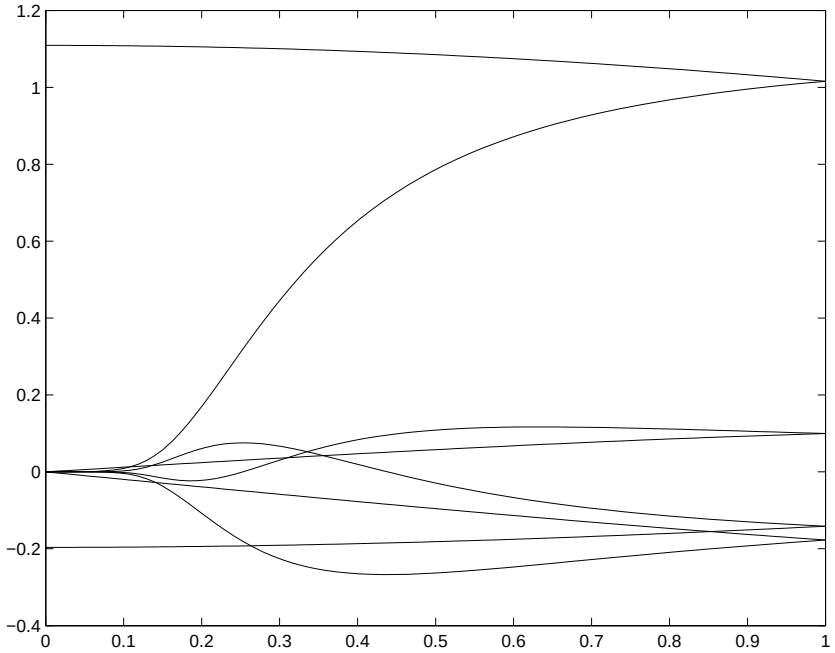

Figure 2.3: Solution of (2.13) computed by `sbvp`.

Finally, we demonstrate that collocation applied to (2.13) shows the expected (empirical) convergence orders. Table 2.1 shows the results for collocation at $m = 4$ equidistant collocation points, the quantities in the table correspond to Table 1.1. As expected, the *stage order* four is observed.

If in contrast we use $m = 4$ Gaussian points as the collocation nodes, we cannot expect to observe superconvergence in general for problems with an essential singularity, see also [6]. Indeed, in this situation an order reduction down to approximately four is observed in Table 2.2.

h_i	err	p
5.0000e−02		
2.5000e−02	3.1006e−05	
1.2500e−02	1.5955e−06	4.28
6.2500e−03	9.1352e−08	4.12
3.1250e−03	5.4666e−09	4.06
1.5625e−03	3.3735e−10	4.01
7.8125e−04	2.1007e−11	4.00

Table 2.1: Convergence order for $m = 4$ equidistant collocation points, problem (2.13).

h_i	err	p
5.0000e−02		
2.5000e−02	3.0001e−06	
1.2500e−02	3.9735e−07	2.91
6.2500e−03	7.8000e−09	5.67
3.1250e−03	4.5092e−10	4.11
1.5625e−03	2.4122e−11	4.22
7.8125e−04	1.4050e−12	4.10

Table 2.2: Convergence order for $m = 4$ Gaussian collocation points, problem (2.13).

Chapter 3

Quasi-Linear Parabolic Equations

3.1 The Original PDEs

Here, we discuss the quasi-linear partial differential equation

$$\frac{\partial u}{\partial t} = \frac{\partial}{\partial x}\left(\left|\frac{\partial u}{\partial x}\right|^{\sigma}\frac{\partial u}{\partial x}\right) + \mathrm{e}^{u}, \tag{3.1}$$

which occurs in turbulent diffusion or the flow of a non-Newtonian fluid, and a related problem which is a model for the temperature profile of a fusion reactor plasma with one source term [30],

$$\frac{\partial u}{\partial t} = \frac{\partial}{\partial x}\left(u^{\sigma}\frac{\partial u}{\partial x}\right) + u^{\beta}. \tag{3.2}$$

In both cases, we prescribe the boundary conditions

$$u(-L,t) = u(L,t) = 0,\ t > 0,\ u(x,0) = u_0(x),\ x \in [-L,L].$$

Here, we consider the cases $\sigma > 0,\ \beta > \sigma + 1$. For $\sigma = 0$, (3.1) is the Frank-Kamenetskii equation (cf. [16]). To study blow-up behavior, the initial function $u_0(x)$ is chosen sufficiently large.

We focus our attention on the problem (3.2) which is also treated numerically in [8]. In [9], qualitative results for (3.1) are derived. The problem does not lend itself to numerical computations readily. Instead, a regularization

$$\frac{\partial u}{\partial t} = \frac{\partial}{\partial x}\left(\left(\left(\frac{\partial u}{\partial x}\right)^{2} + \varepsilon^{2}\right)^{\sigma/2}\frac{\partial u}{\partial x}\right) + \mathrm{e}^{u},$$

where $\varepsilon = 10^{-6}$, could be used. For this problem, self-similarity is not retained and the approach described in this report is not feasible. We do not give details here.

3.2 Associated ODEs

The differential equation (3.1) is invariant under the Lie group of transformations

$$t \to \lambda t,\ x \to \lambda^{1/(\sigma+2)}x,\ u \to u - \log(\lambda),$$

while the same holds for (3.2) for

$$t \to \lambda t,\ x \to \lambda^m x,\ u \to \lambda^{-1/(\beta-1)} u,$$

where $m = 1/2 - \sigma/(2\beta - 2) > 0$.

The self-similar solutions which are invariant under these transformations take the form

$$u(x,t) = -\log(T-t) + z(\tau) \quad \text{with } \tau = \frac{|x - x_*|}{(T-t)^{1/(\sigma+2)}}$$

and

$$u(x,t) = \frac{z(\tau)}{(T-t)^{1/(\beta-1)}} \quad \text{with } \tau = \frac{|x - x_*|}{(T-t)^m},$$

respectively. For both equations, $x_* \in (-L, L)$ denotes the point where blow-up occurs.

Substitution of the respective ansatz into the differential equation (3.1) or (3.2) yields the ordinary differential equations

$$(|z'(\tau)|^\sigma z'(\tau))' - \frac{\tau}{\sigma+2} z'(\tau) + \mathrm{e}^{z(\tau)} - 1 = 0, \quad \tau > 0, \tag{3.3}$$

and

$$(z^\sigma(\tau) z'(\tau))' - m\tau z'(\tau) - \frac{1}{\beta-1} z(\tau) + z^\beta(\tau) = 0, \quad \tau > 0. \tag{3.4}$$

Symmetry yields the boundary condition

$$z'(0) = 0.$$

Moreover, matching conditions corresponding to the boundary conditions for the original PDEs are prescribed for the self-similar solutions. These are respectively

$$\lim_{\tau\to\infty} z(\tau) + (\sigma+2)\log(\tau) = C,$$

and

$$\lim_{\tau\to\infty} z(\tau)\tau^{1/m(\beta-1)} = C,$$

where C is a suitable constant in each case. This means that in general it is required that z is "slowly-growing" rather than bounded for $\tau \to \infty$. Consequently, the problem does not fit into the context of the treatment in [19], [24], [25] and consequently [20]. Only for problem (3.4) with the choice of parameters $\beta > \sigma + 1 > 1$, the resulting problem fits into our framework, and can be solved successfully by transformation to a finite interval. Details are given in [22].

3.3 Numerical Solution

In [8], a shooting method is used to solve the problem (3.4). The initial value $z(0) = \alpha$ is varied slowly until slowly growing solutions are encountered at some point $\mathcal{T} \approx 10$. The initial value problems are solved using a BDF solver from the package DDASSL, see [26].

To solve the singular problem resulting from the transformation of (3.4) to a finite interval analogously as in the previous chapters, a collocation solver for implicit, second-order ODEs was implemented. The details of the procedure and the advantageous numerical properties of our approach are discussed in [22].

Chapter 4

The Complex Ginzburg-Landau Equation

4.1 The Original PDE

The complex Ginzburg-Landau equation

$$\mathrm{i}\frac{\partial u}{\partial t} + (1 - \mathrm{i}\varepsilon)\Delta u + (1 + \mathrm{i}\delta)|u|^2 u = 0, \quad t > 0, \tag{4.1a}$$

$$u(x, 0) = u_0(x), \quad x \in \mathbb{R}^d \tag{4.1b}$$

arises as a model in a variety of problems from physics, biology and chemistry. These include nonlinear optics, models of turbulence, Rayleigh-Benard convection, superconductivity, superfluidity, Taylor-Couette flow and reaction-diffusion systems, see for example [1].

Equation (4.1) is a perturbed version of the nonlinear Schrödinger equation (1.1) when ε and δ are small. Self-similar blow-up solutions for this case are studied in [11]. It turns out that the monotone solution, as well as the unstable multi-bump solutions of (1.1) have corresponding solution branches when the perturbation parameters are varied. In addition, stable non-monotone solutions exist for (4.1) which can be obtained from solutions of (1.1) by pathfollowing past a turning point. For details, see [11] and [27].

4.2 Associated ODE and Transformed Problem

It is demonstrated in [11] that the self-similar solutions of (4.1) obey the same scaling laws as for (1.1). A similarity reduction analogous (but unequal) to (1.4) yields a perturbed version of (1.5),

$$(1-\mathrm{i}\varepsilon)\left(z''(\tau) + \frac{d-1}{\tau}z'(\tau)\right) - z(\tau) + \mathrm{i}a(\tau z(\tau))' + (1+\mathrm{i}\delta)|z(\tau)|^2 z(\tau) = 0, \quad \tau > 0, \tag{4.2}$$

with the same boundary conditions

$$z'(0) = 0, \quad \Im z(0) = 0, \quad \lim_{\tau\to\infty} \tau z'(\tau) = 0. \tag{4.3}$$

The same transformations as in Section 1.3 again yield the singular boundary value problem (1.18), where

$$M(\tau) = \begin{pmatrix} 0 & 1 \\ \tau^2 \frac{1+\varepsilon a+\mathrm{i}(\varepsilon-a)}{1+\varepsilon^2} & 2-d+\tau^2 \frac{\varepsilon a-\mathrm{i}a}{1+\varepsilon^2} \end{pmatrix},$$

$$f(\tau, z) = \begin{pmatrix} 0 \\ \tau \frac{\varepsilon\delta-1-\mathrm{i}(\varepsilon+\delta)}{1+\varepsilon^2} z_1 |z_1|^2 \end{pmatrix},$$

$$A(\tau) = \begin{pmatrix} 0 & -\tau^2 \\ -\frac{1+\varepsilon a+\mathrm{i}(\varepsilon-a)}{1+\varepsilon^2} & \frac{\mathrm{i}a-\varepsilon a}{1+\varepsilon^2} - \tau^2(2-d) \end{pmatrix},$$

$$g(\tau, z_3, z_4) = \begin{pmatrix} 0 \\ -\frac{1}{\tau^3} \frac{\varepsilon\delta-1-\mathrm{i}(\varepsilon+\delta)}{1+\varepsilon^2} z_3 |z_3|^2 \end{pmatrix}.$$

Again, we prescribe the boundary conditions (1.19).

4.3 Numerical Solution

In order to approximate the solutions of (4.2), we set $\delta = \varepsilon$ and use pathfollowing starting at $\varepsilon = 0$ (that is, at the solutions of the nonlinear Schrödinger equation). To observe some of the more interesting stable solutions, continuation based on pseudo-arclength parametrization will be necessary to pursue the solution branches across turning points. Here, we merely demonstrate that using `sbvp` we can in principle solve the equations (4.2) (in the form of the singular ODEs of the first order) for some fixed values of ε which constitute a small perturbation of (1.5) and can be solved using the solution of (1.5) (or rather, (1.18) in practice) as starting values. In Figures 4.1–4.5, we give the resulting solution profiles for $\varepsilon = 10^{-6}$, 10^{-5}, 10^{-4}, 10^{-3} and 10^{-2}. Table 4.1 gives the values of the maximal difference diff between the solutions of the nonlinear Schröedinger equation (1.18) and the complex Ginzburg-Landau equation for the respective values of ε. We observe that the solution of (4.2) appears to depend relatively smoothly on the perturbation parameter within the considered range, the difference as compared with the solutions of the nonlinear Schrödinger equation grows monotonely with ε.

ε	10^{-6}	10^{-5}	10^{-4}	10^{-3}	10^{-2}
diff	0.0422	0.3851	1.9139	2.1898	4.1810

Table 4.1: Difference between the solutions of (4.2) and (1.5) for some values of ε.

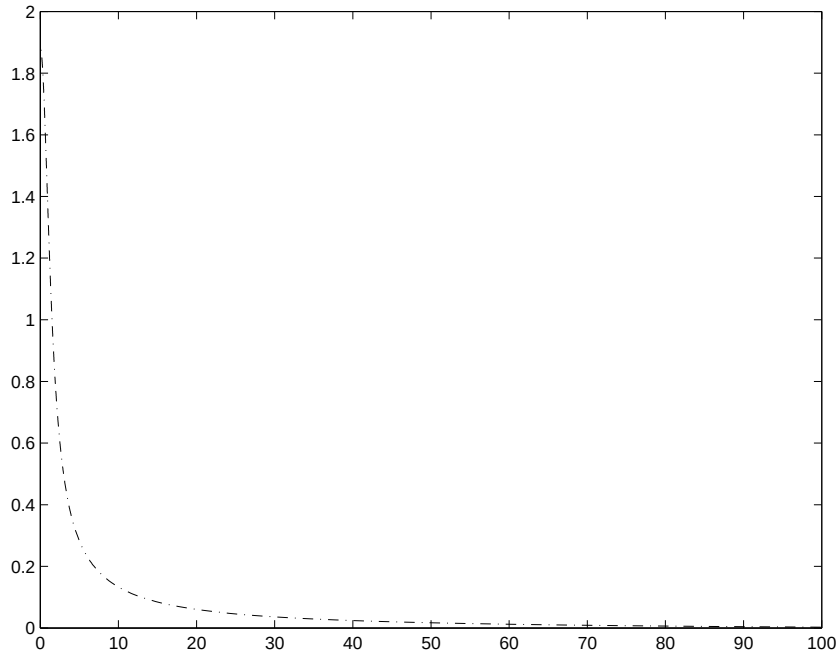

Figure 4.1: Solution profile of (4.2) for $\varepsilon = 10^{-6}$.

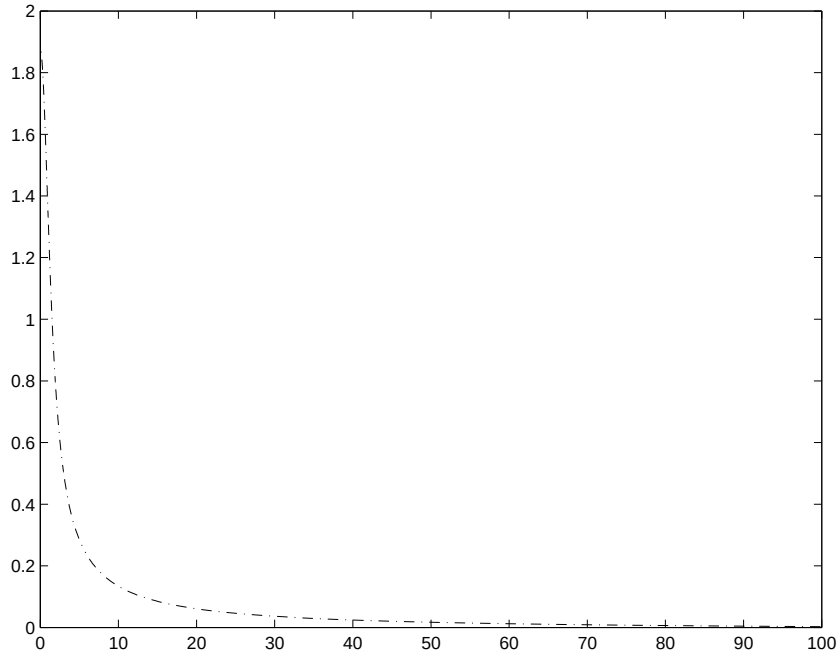

Figure 4.2: Solution profile of (4.2) for $\varepsilon = 10^{-5}$.

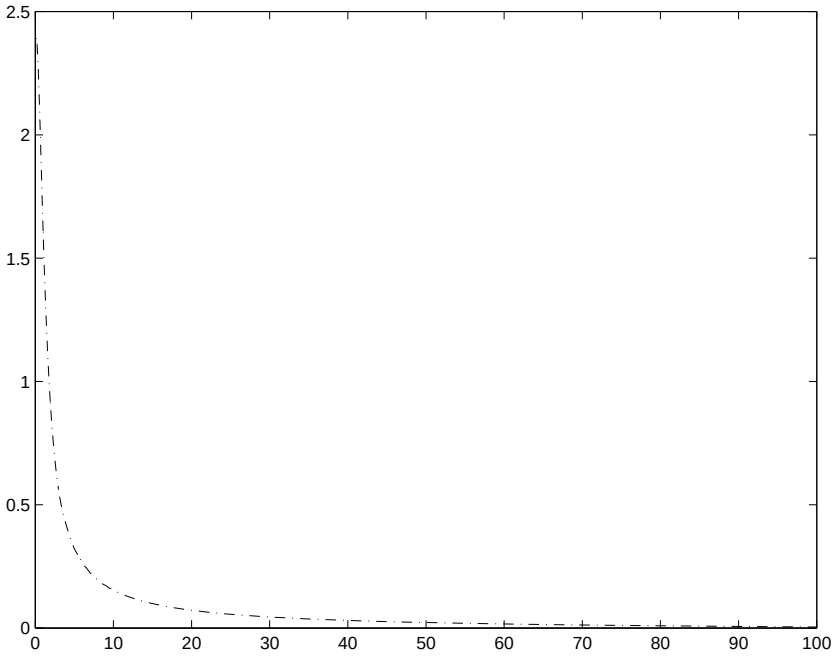

Figure 4.3: Solution profile of (4.2) for $\varepsilon = 10^{-4}$.

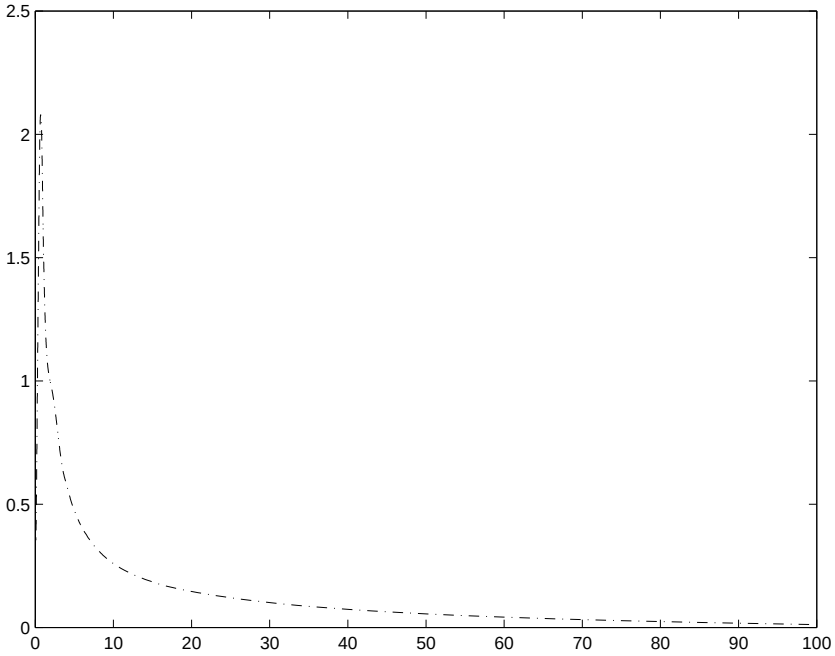

Figure 4.4: Solution profile of (4.2) for $\varepsilon = 10^{-3}$.

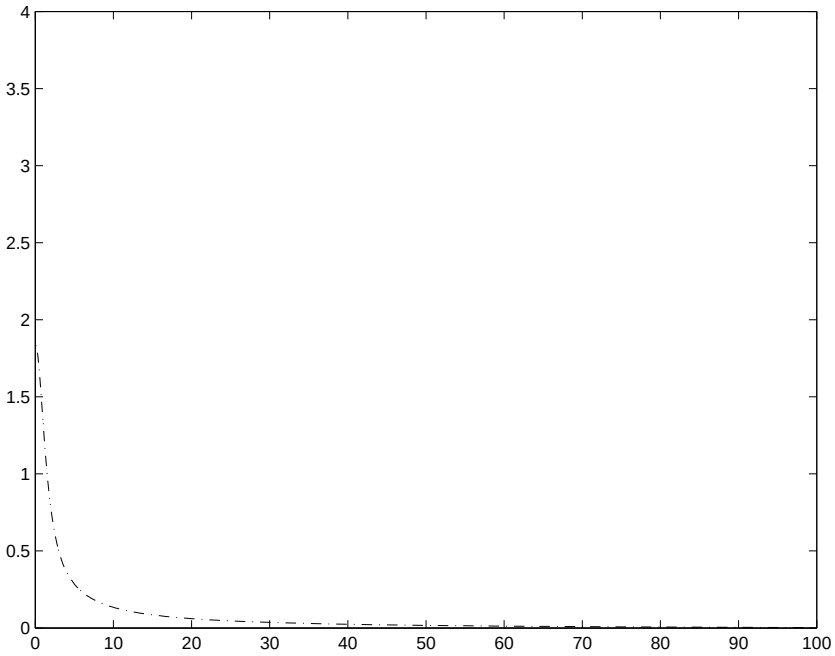

Figure 4.5: Solution profile of (4.2) for $\varepsilon = 10^{-2}$.

References

[1] S. Aranson, I. L. Kramer: *The World of the Complex Ginzburg-Landau Equation*. Rev. Mod. Phys. 74 (2002), pp. 99–143.

[2] U. Ascher, J. Christiansen, R. D. Russell: *Collocation Software for Boundary Value ODEs*. ACM Transactions on Mathematical Software 7 (1981)(2), pp. 209–222.

[3] W. Auzinger, G. Kneisl, O. Koch, E. Weinmüller: *A Collocation Code for Boundary Value Problems in Ordinary Differential Equations*. Numer. Algorithms 33 (2003), pp. 27–39.

[4] W. Auzinger, D. Koch, O. Praetorius, E. Weinmüller: *New a Posteriori Error Estimates for Singular Boundary Value Problems*. Submitted to Numer. Algorithms. Also available at `http://www.math.tuwien.ac.at/~inst115/preprints.htm/`.

[5] W. Auzinger, O. Koch, E. Weinmüller: *Analysis of a New Error Estimate for Collocation Methods Applied to Singular Boundary Value Problems*. To appear in SIAM J. Numer. Anal. Also available at `http://www.math.tuwien.ac.at/~inst115/preprints.htm/`.

[6] W. Auzinger, O. Koch, E. Weinmüller: *Collocation Methods for Boundary Value Problems with an Essential Singularity*. In *Large-Scale Scientific Computing* (I. Lirkov, S. Margenov, J. Wasniewski, P. Yalamov, eds.), Springer Verlag, Vol. 2907 of *Lecture Notes in Computer Science*, pp. 347–354.

[7] M. Ben-Artzi, H. Koch, C. J. Saut: *Dispersion Estimates for Fourth Order Schrödinger Equations*. C. R. Acad. Sci. Paris Série I Math 330 (2000), pp. 87–92.

[8] C. Budd, J. Chen, V. A. Galaktionov: *Focusing Blow-Up for Quasilinear Parabolic Equations*. Proc. R. Soc. Edinb. 128A (1998), pp. 965–992.

[9] C. Budd, V. A. Galaktionov: *Stability and Spectra of Blow-Up in Problems with Quasi-Linear Gradient Diffusivity*. Proc. R. Soc. Lond. A 45A (1998), pp. 2371–2407.

[10] C. Budd, V. A. Galaktionov, J. F. Williams: *Self-Similar Blow-Up in Higher-Order Semilinear Parabolic Equations*. Preprint 02/10, Dept. Math. Sci., Univ. of Bath, 2002.

[11] C. J. Budd, V. Rottschäfer, J. F. Williams: *Multi-Bump, Blow-Up, Self-Similar Solutions of the Complex Ginzburg-Landau Equation*. Submitted to Nonlinearity.

[12] C. J. Budd: *Asymptotics of multibump blow-up self-similar solutions of the nonlinear Schrödinger equation*. SIAM J. Appl. Math. 62 (2001)(3), pp. 801–830.

[13] C. J. Budd, S. Chen, R. D. Russell: *New Self-Similar Solutions of the Nonlinear Schrödinger Equation with Moving Mesh Computations*. J. Comput. Phys. 152 (1999), pp. 756–789.

[14] E. J. Doedel: *Auto, a Program for the Automatic Bifurcation Analysis of Autonomous Systems*. Cong. Numer. 30 (1981), pp. 265–384.

[15] G. Fibich, B. Ilan, G. Papanicolau: *Self-Focusing with Fourth-Order Dispersion*. SIAM J. Appl. Math. 62 (2002), pp. 1437–1462.

[16] D. A. Frank-Kamenetskii: *Towards Temperature Distributions in a Reaction Vessel and the Stationary Theory of Thermal Explosion*. Doklady Akad. Nauk SSSR 18 (1938), pp. 411–412.

[17] A. Hasegawa: *Optical Solitons in Fibers*. Springer Verlag, Berlin, 1989.

[18] F. R. d. Hoog, R. Weiss: *Difference Methods for Boundary Value Problems with a Singularity of the First Kind*. SIAM J. Numer. Anal. 13 (1976), pp. 775–813.

[19] F. R. d. Hoog, R. Weiss: *An Approximation Theory for Boundary Value Problems on Infinite Intervals*. Computing 24 (1980), pp. 227–239.

[20] F. R. d. Hoog, R. Weiss: *On the Boundary Value Problem for Systems of Ordinary Differential Equations with a Singularity of the Second Kind*. SIAM J. Math. Anal. 11 (1980), pp. 41–60.

[21] G. Kitzhofer: *To be announced*. Ph.D. Thesis, Inst. for Anal. and Sci. Computing, Vienna Univ. of Technology, Austria, 2004. In preparation.

[22] G. Kitzhofer, O. Koch, E. Weinmüller: *Kollokationsverfahren für singuläre Randwertprobleme zweiter Ordnung in impliziter Form*. Techn. Rep. ANUM Preprint Nr. 9/04, Inst. for Anal. and Sci. Comput., Vienna Univ. of Technology, Austria, 2004. Available at `http://www.math.tuwien.ac.at/~inst115/preprints.htm`.

[23] O. Koch: *Asymptotically Correct Error Estimation for Collocation Methods Applied to Singular Boundary Value Problems*, 2003. Submitted to Numer. Math. Available at `http://www.othmar-koch.org/research.html`.

[24] M. Lentini, H. Keller: *Boundary Value Problems on Semi-Infinite Intervals and Their Numerical Solution*. SIAM J. Numer. Anal. 17 (1980)(4), pp. 577–604.

[25] P. A. Markowich: *Analysis of Boundary Value Problems on Infinite Intervals*. SIAM J. Math. Anal. 14 (1983), pp. 11–37.

[26] L. Petzold: *A Description of DASSL: A Differential Algebraic System Solver*. Report SAND82-8637, Amer. Math. Soc., Sandia National Labs, 1982.

[27] P. Plecháč, V. Šverák: *On Self-Similar Singular Solutions of the Complex Ginzburg-Landau Equation*. Comm. Pure Appl. Math. 54 (2001), pp. 1215–1242.

[28] L. Shampine, J. Kierzenka: *A BVP Solver Based on Residual Control and the MATLAB PSE*. ACM T. Math. Software 27 (2001), pp. 299–315.

[29] V. E. Zakharov: *Handbook of Plasma Physics*, Vol. 2. Elsevier, New York, 1984.

[30] N. V. Zmitrenko, S. P. Kurdyumov, A. P. Mikhailov, A. A. Samarskii: *Localization of Thermonuclear Combustion in a Plasma with Electronic Thermal Conductivity*. JETF Lett. 26 (1977), pp. 469–472.